Band Positions of Anatase (001) and (101) Surfaces in Contact with Water from Density Functional Theory

Julian Geiger,[1,2] Michiel Sprik,[1,a)] and Matthias M. May[1,3]

[1)]*Department of Chemistry, University of Cambridge, United Kingdom*

[2)]*Friedrich-Alexander University Erlangen-Nürnberg, Germany*[b)]

[3)]*Institute for Solar Fuels, Helmholtz-Zentrum Berlin für Materialien und Energie GmbH, Germany*[c)]

(Dated: 25 April 2020)

Titanium dioxide in the anatase configuration plays an increasingly important role for photo(electro)catalytic applications due to its superior electronic properties when compared to rutile. In aqueous environments, the surface chemistry and energetic band positions upon contact with water determine charge-transfer processes over solid–solid or solid–electrolyte interfaces. Here, we study the interaction of anatase (001) and (101) surfaces with water and the resulting energetic alignment by means of hybrid density functional theory. While the alignment of band positions favours charge-transfer processes between the two facets for the pristine surfaces, we find the magnitude of this underlying driving force to crucially depend on water coverage and degree of dissociation. It can be largely alleviated for intermediate water coverages. Surface states and their passivation by dissociatively adsorbed water play an important role here. Our results suggest that anatase band positions can be controlled over a range of almost one eV via its surface chemistry.

[a)]Electronic mail: ms284@cam.ac.uk

[b)]Present address: Institut Català d'Investigació Química, Tarragona, Spain

[c)]Present address: Institute of Theoretical Chemistry, Ulm University, Germany

I. INTRODUCTION

Titania (TiO$_2$) is one of the most prominent materials in (electro)catalysis, notably in the function as a photocatalyst or protection layer for solar water splitting.[1,2] Here, the application case crucially depends on the energetic alignment of the bands with respect to the electrolyte or the underlying photoabsorber. Furthermore, titanium dioxide is the model system par excellence for a wide-gap metal-oxide to study the electronic properties of a semiconductor in contact with water, both experimentally[3–5] and theoretically,[4,6–16] hereby also playing an important role in method development and validation.

Anatase is, though metastable, considered the more interesting polymorph of TiO$_2$ for photocatalysis as it exhibits superior electronic properties, manifested in longer charge-carrier lifetimes when compared to rutile.[17] In a density functional theory (DFT)-based molecular dynamics study, evidence was found for a trapping mechanism of excess electrons on the anatase (101) surface, whereas the (001) surface acts as hole acceptor.[12] Experimentally, photoelectron spectroscopy at differently treated (101) and (001) surfaces of single-crystals evidenced a band offset favouring electron migration to the (101) facets, whose magnitude depends on prior sample treatment.[18,19] Such a driving force could help in improving the catalytic activity of TiO$_2$ nanoparticles or improve the charge-transport over hetero-interfaces for TiO$_2$-based protection layers. A key question, to be addressed in this study, is to what extent the contact with water modifies this surface electronic structure behaviour.

In this work we have considered the (101) and (001) surfaces of anatase, as illustrated in Fig. 1. The (101) surface is characterised by a ridge-like structure with every second titanium atom being coordinatively saturated and buried in the trenches of the surface steps. The other half entail a five-fold coordination, exposing one free coordination site that can function as anchoring point for adsorbate molecules. In contrast, all titanium and half of the oxygen atoms constituting the (001) surface are coordinatively unsaturated, with the uppermost oxygen atoms bearing large bond angles of around 150°. The high degree of unsaturation and the strained bonding situation lead to the well-known increased reactivity of this surface. It can undergo reconstruction under ultra-high vacuum conditions,[20] yet also the unreconstructed surface has been observed.[19] As adsorption of water prevents reconstruction in an aqueous environment,[21,22] the slab models employed in this work correspond to the unreconstructed surface.
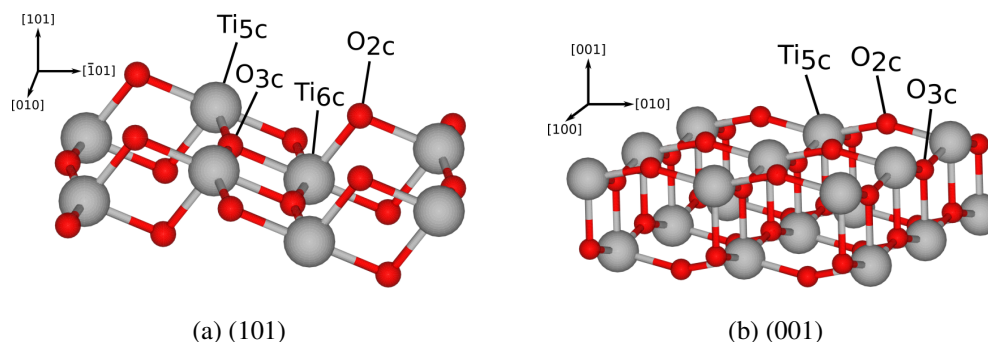
FIG. 1. Ball-and-stick models of the atomic upper layers for the considered anatase surfaces.

Experimental and theoretical work on the initial water layer in contact with anatase surfaces found a mixture of dissociative and molecular adsorption, with temperatures beyond 120 K initiating dissociation on (101) surfaces.[5] Furthermore, intermediate water coverages are believed to lower the dissociation barrier.[23] Slow adsorption at low temperatures, can, however, result in the formation of an ordered, full coverage of molecular water.[5] A detailed insight into the interplay between surface chemistry and surface electronic states is required to understand the interfacial energetic alignment between solid and electrolyte, as well as different facets of anatase (nano)crystals.

Here, we present electronic structure calculations of titanium dioxide surfaces in the anatase structure, investigating the energetic band alignment with and without (fractional) water coverage. We find that facet-driven charge-carrier separation is favoured in a static picture by band-offset. However, band positions can be modified significantly through the adsorption of water. The magnitude of the surface chemistry-induced shifts of the band levels depends on coverage and degree of dissociation and can be in the order of up to one eV.

II. METHODS

We performed DFT electronic ground state calculations with the CP2K code,[24] employing the Gaussian-And-Plane-Wave scheme with GTH pseudopotentials. The Gaussian basis sets were of double-ζ quality[25] and an energetic cutoff of 600 Ry was used. Initial optimisations of our slabs were carried out within the generalised gradient approach (GGA), using the PBE functional.[26,27] The resulting structures were then subjected to further relaxation with the HSE06 hybrid functional, using the auxiliary density matrix method as implemented in CP2K.[28,29] In the subsequent

73 hybrid functional optimisations, all atoms were allowed to relax further, while keeping the cell

74 sizes fixed at the PBE-calculated values. Total energies were evaluated at the Γ-point. For the

75 (001) surface, the in-plane dimensions of our model systems comprised four unit cells in x- and

76 y-direction, extending 15.08 Å in each direction. The (101) surface was modeled by supercells

77 composed of one unit cell in x- and three in y-direction, corresponding to dimensions of 10.26 Å

78 and 11.31 Å, respectively. The slabs were separated by 20 Å of vacuum along the z-direction. No

79 constraints on atomic positions were applied and the full slabs were allowed to relax. For the ge-

80 ometry optimisations, we first optimised the crystal-structures in vacuum, with, in the case of the

81 water-covered surfaces, a subsequent further relaxation after addition of 0.25 (in the case of the

82 (001) surface), 0.5, or 1.0 monolayers (ML) of water. Water molecules were initially positioned

83 on the surfaces in a way to facilitate coordination of the oxygen atoms to the under-coordinated

84 titanium atoms and to allow for hydrogen bonding with the surface oxygen atoms.[30,31] Based on

85 full ML coverage, removal of certain water molecules resulting in high-symmetry over-structures

86 provided starting points for optimisations with sub-ML coverages. Additionally, we varied the

87 number of Ti-layers along the z-direction between 8 and 20 to investigate band gap convergence

88 and to confirm the absence of any intrinsic dipole of the surfaces. For these considerations we ap-

89 plied the PBE functional and, in the case of the (001) surface, a smaller 3 by 3 supercell. Presented

90 surface structures, band gap values, adsorption energies, heats of formation and partial densities of

91 states (PDOS) were obtained using slabs with 20 Ti-layers in the z-direction and the HSE06 hybrid

92 functional. These structures were chosen to be in a well-converged regime for band positions and

93 energy gaps, as confirmed beforehand.

III. RESULTS AND DISCUSSION

95 The main structures resulting from our geometry optimisations for the different water coverages

96 are shown in Figs. 2 and 3 and Supplementary Figs. 1 and 2. Irrespective of the coverage, we obtain

97 only molecular adsorption on the (101) surface. This is consistent with previous reports,[31] in which

98 molecular adsorption was identified as energetically favourable over dissociative adsorption. In

99 the resulting structures, the water molecules are coordinated to the surface titanium atoms and

100 hydrogen bonds to the surface oxygen atoms are formed.

101 For full ML coverage on the (001) surface, on the other hand, we observe partial dissociation,

102 as shown in Fig. 3a. The resulting structure is similar to a previously reported result,[7] in which

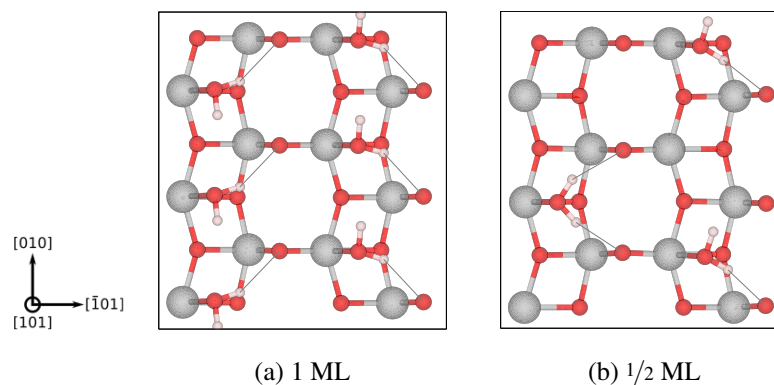[010]
[101]
[101]

(a) 1 ML   (b) ½ ML

FIG. 2. Top view of water adsorbed on the (101) surface, with one (a) and half a monolayer (b) coverage. Hydrogen bonds are represented as thin grey lines.

adsorption of one ML of water on the (001) surface led to the dissociation of one quarter of the water molecules. The remaining molecularly adsorbed water forms complex networks of hydrogen bonds, also including surface oxygen atoms. This structure was obtained after application of the HSE06 hybrid functional, whereas initial optimisation with PBE resulted in an ordered, fully non-dissociated, adsorbed layer of water. For half ML coverage, we observed mixed molecular and dissociative adsorption, Fig. 3b, while quarter ML coverage led to fully dissociative adsorption, Fig. 3c. In both of these cases, the resulting total number of surface hydroxyl groups is the same. Dissociative water adsorption presents an energetically favourable process, as it alleviates some of the strain caused by the large bond angles around the oxygen atoms present in the pristine surface. The final structures are further stabilised by hydrogen bonds between the surface hydroxyl groups, if present, also including the molecularly adsorbed water. Interestingly, the geometric motif around the pairs of surface hydroxyl groups shows a close similarity to the common 1 x 4 reconstruction of the pristine (001) surface, as previously reported.[7]

Mixed dissociative adsorption of water on the (001) surface allows for the formation of various geometrically distinct final structures, differing in the relative positioning of the resulting surface hydroxyl groups. While we have not realized an extensive search over these geometrically distinct structures, we have considered various representative examples for each water coverage. We found their differences in relative stability, water adsorption energy and electronic structure to be negligible. Experimentally, we expect them, in principle, to be distinguishable by surface-sensitive methods such as low-energy electron diffraction. However, for real surfaces at finite temperatures,
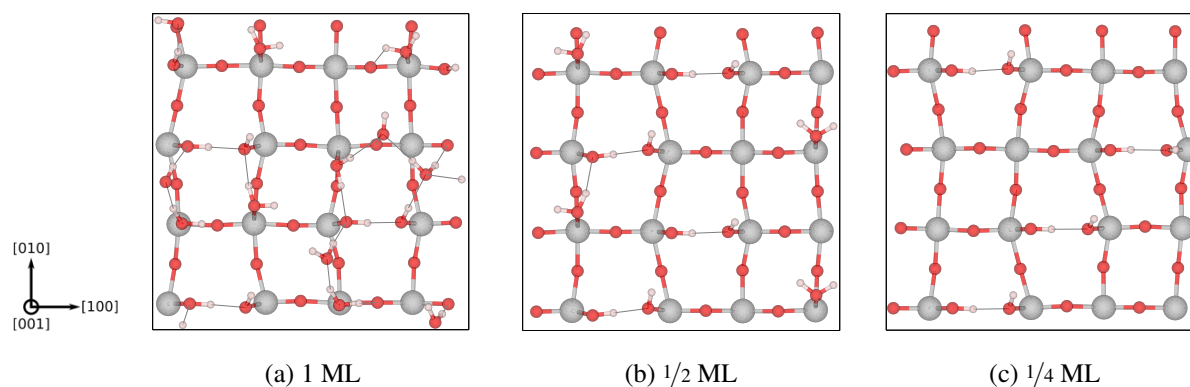
Band Positions of Anatase by DFT

(a) 1 ML   (b) ½ ML   (c) ¼ ML

FIG. 3. Top view of mixed (a,b) and fully dissociative (c) water adsorption on the (001) surface from different water coverages.

124 different superstructures might co-exist.

125 To assess stability and likelihood of actual occurrence, we calculated heat of formation energies,

126 $\Delta H_f(\theta)$, and adsorption energies, E_{ads}, as a function of the coverage, θ. The resulting values per

127 (1×1) surface unit cell are listed in Table I for different coverages and different degrees of disso-

128 ciation. The heat of formation energy as a measure for relative stability is obtained from the total

129 energies, E^{tot}, neglecting the pV term and vibrational energies,[32] as follows:

$$\Delta H_f(\theta) = E^{tot}(\theta) - E^{tot}(0) - \theta \left[E^{tot}(1) - E^{tot}(0) \right]. \tag{1}$$

131 Adsorption energies per water molecule were calculated as:

$$E_{ads} \cdot n_{H_2O} = E^{tot}(\theta) - \left[E^{tot}(0) + n_{H_2O} \cdot (E^{tot}_{H_2O,g}) \right], \tag{2}$$

133 with the total energy of a single gas-phase water molecule, $E^{tot}_{H_2O,g}$, and the number of water

134 molecules, n_{H_2O}. In general, our values of the adsorption energies show a similar trend as reported

135 in the literature.[22,31] For the (001) surface, the most favourable structure at a quarter of a ML is

136 a fully dissociated adsorption of water molecules, while for 0.5 ML, half of the water molecules

137 stay intact, leading to a comparable heat of formation.

138

139 Densities of states for the (001) surface with different water coverages are shown in Fig. 4. It

140 should be noted that the seemingly large magnitude of the band gaps is due to the fact that the

141 lowest unoccupied states are too small to be visible in this representation. However, they lie in fact

142 about 3.2 eV to 3.6 eV above the valence band maximum, as expected. Analysis of the density

Band Positions of Anatase by DFT

TABLE I. Heat of formation energies (per surface unit cell) and adsorption energies (per water molecule). Different degrees of dissociation are labelled as fd: fully dissociated, pd: partially dissociated, and ud: undissociated.

(001) surface

Water coverage / ML	E_{ads} / eV	ΔH_f / eV
0.25 fd	-2.34	-0.35
0.25 pd	-1.92	-0.25
0.5 pd	-1.43	-0.25
1.0 pd	-0.94	0.00

(101) surface

0.5	-0.77	-0.04
1.0	-0.73	0.00

of states shows that the pristine (001) surface exhibits an occupied Ti-related surface state in the band gap region close to the valence band maximum, which reduces the effective band gap. It can be seen in Fig. 4a) and is clearly visible in the local density of states of the very top Ti-O layer (Supplementary Fig. 3). This occupied surface state leads to a charge redistribution between surface and bulk, hereby contributing to the shift of band positions (see below). However, dissociative adsorption of water causes the disappearance or a 'passivation' of this state, as can be seen in Fig. 4b,c. For the (101) surface, this state is absent, resulting in virtually unchanged Ti-related valence band features and a constant band gap.

This is similar to the experimental photoelectron spectroscopy results of Kashiwaya *et al.*[18]: Their study on differently prepared single-crystals of anatase with X-ray and ultraviolet photoemission in vacuum find occupied surface states slightly above the bulk valence band maximum for the (001) surface that can be – apart from a shallow valence band surface state – largely suppressed by dedicated sputter-annealing routines followed by reoxidation. Their (001) surface without reoxidation still comprises a deep band gap state very close to the middle of the band gap. Though they consider this type of surface "stoichiometric", our results show that the occupied surface state for the pristine (001) surface is very close to the highest occupied bulk states. Consequently, the signatures of their "oxidised" surface are closer to the pristine, unreconstructed surface. In the
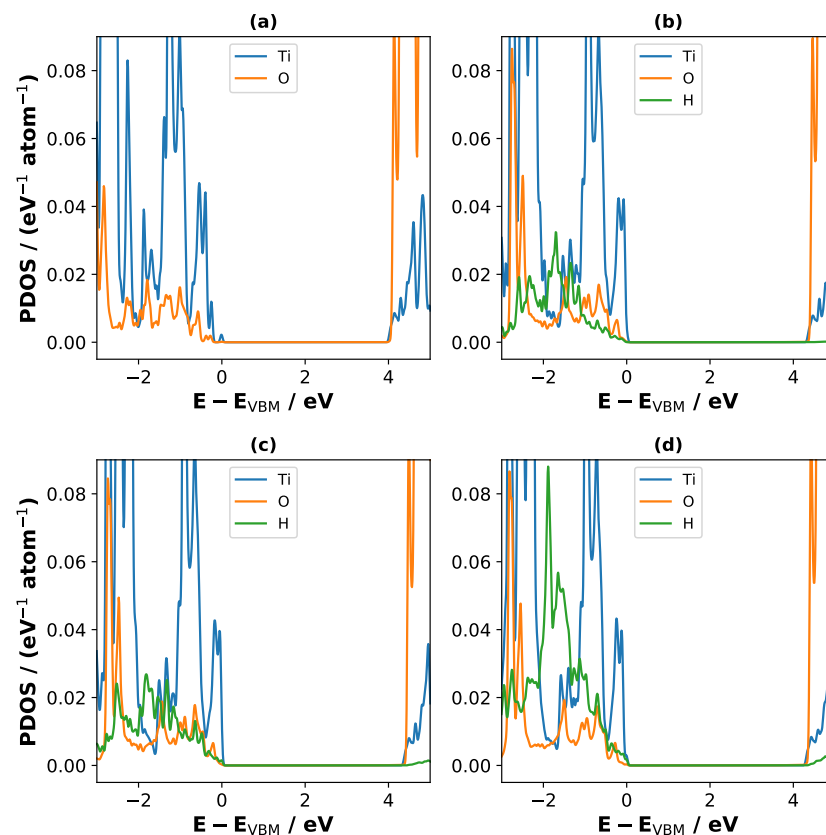
FIG. 4. Partial density of states (PDOS) for the lowest-energy (001) surfaces. (a) without water, (b) with a quarter ML of fully dissociated water, (c) with half a ML of partially dissociated , and (d) with a full ML of partially dissociated water. Energies are referred to the valence band maximum, E_{VBM}.

160 case of the (101) surface, the "stoichiometric" samples would indeed correspond to the pristine

161 configuration, which means that the annealing procedure creates oxygen vacancies that have to be

162 cured by dedicated oxidation.

163

164 The band gaps of the different structures are presented in Fig. 5. These were obtained by tak-

165 ing the difference between the conduction band minimum (CBM) and the valence band maximum

166 (VBM) for each system. As expected, the gaps for the (101) surface are with 3.64 eV largest and

167 virtually unaffected by water in the vicinity of the surface. This value represents the well-known,

168 slight overestimation of HSE06 in comparison to the experimental band gap.[33] The picture for

169 the (001) surface is, however, a completely different one. The pristine, unreconstructed surface

170 shows a reduced gap of 3.24 eV, which can be attributed to the previously discussed surface state.

171 The band gap continuously increases with the number of dissociatively adsorbed water molecules.

172 While partial dissociation of a quarter ML yields a value of 3.32 eV, about 80 meV above the

173 gap of the pristine surface, fully dissociative adsorption causes a strong increase to 3.57 eV, over

174 330 meV above the pristine surface. In the case of partial dissociation of half a ML of water, the

175 total concentration of surface hydroxyl group is the same. Thus, the band gap for this system is

176 with 3.59 eV nearly identical. These values almost reach the band gap magnitude of the (101)
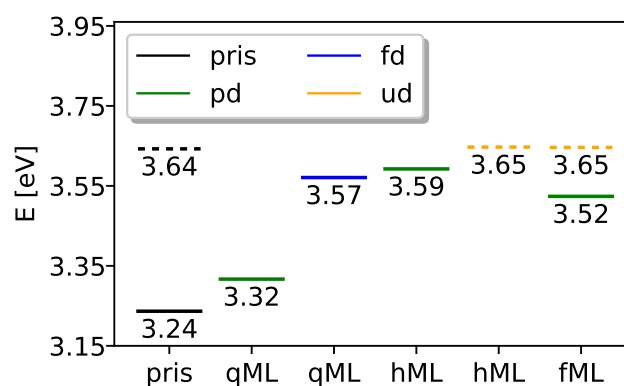
177 surface.

178

FIG. 5. Band gaps for (001) and (101) surfaces of anatase, represented as solid and dashed lines, respectively. Different degrees of water dissociation are indicated by different colouring.

179   More relevant for charge-transfer processes between crystal facets or to electrolytes are, how-

180 ever, the relative and absolute energetic positions of valence and conduction bands. To obtain

181 the absolute energetic positions of the VBM and CBM, we subtracted the Hartree potential in

182 the vacuum region, projected onto the *z*-axis, from the HOMO and LUMO energies of the DFT

183 calculations. This referencing has initially no physical meaning in a 3D periodic calculation.

184 However, as the vacuum level of the Hartree potential is dependent on the crystal-to-vacuum ratio,

185 it converges to a specific value with the number of layers (not shown here). Thus, the dependency

186 on the number of layers in the crystal – keeping the amount of vacuum fixed – cancels and the

187 obtained values quickly converge with slab thickness.

188

189 Figure 6 shows the resulting band positions with respect to the Hartree potential at vacuum

190 for each system. For the pristine surfaces, the CBM of the (101) surface lies 600 meV lower

191 than for the (001) surface. With a value of 1 eV, this difference is even more pronounced for the

192 VBM. In a nanocrystal, where both surfaces can be present on different facets, the band position

193 difference of the two facets represents an intrinsic driving force for electron-hole separation after
194 photoexcitation.[12] The hole should be more stable in the (001) system, whereas the electrons
195 will be trapped in the lower energy levels of the (101) conduction band. However, we find that
196 the electronic structures of the surfaces exposed by such a nanocrystal can be influenced con-
197 siderably by the presence of water. While dissociative adsorption on the (001) surface mainly
198 causes a decrease of the VBM level, molecular adsorption on both surfaces leads to an almost
199 linear increase of both band positions. This is especially evident in the case of the (101) surface,
200 where the band levels for the fully covered surface lie about $1.3 \, \mathrm{eV}$ higher than for the pristine
201 surface. The resulting position of the CBM at $-3.75 \, \mathrm{eV}$, as compared to a value of $-4.02 \, \mathrm{eV}$ for
202 the fully covered (001) surface, suggests a higher stability of electrons in the (001) surface. This
203 stands in contrast to the previously mentioned trapping of electrons at the (101) facets. Similarly,
204 coverage of half a ML of water causes the band positions of both surfaces to approach values of
205 about $-7.9 \, \mathrm{eV}$ (VBM) and $-4.3 \, \mathrm{eV}$ (CBM), again reducing the driving force for electron-hole
206 separation. Comparison of different coverages and degrees of dissociation for both surfaces,
207 however, shows that the intrinsic band level differences between the two surfaces can also be
208 further increased. For instance, full ML coverage on the (001) surface leads to an overall increase
209 of band positions and therefore enhances the band level differences to the pristine (101) surface.
210 This should in turn further improve the efficiency of electron-hole separation after photoexcitation.
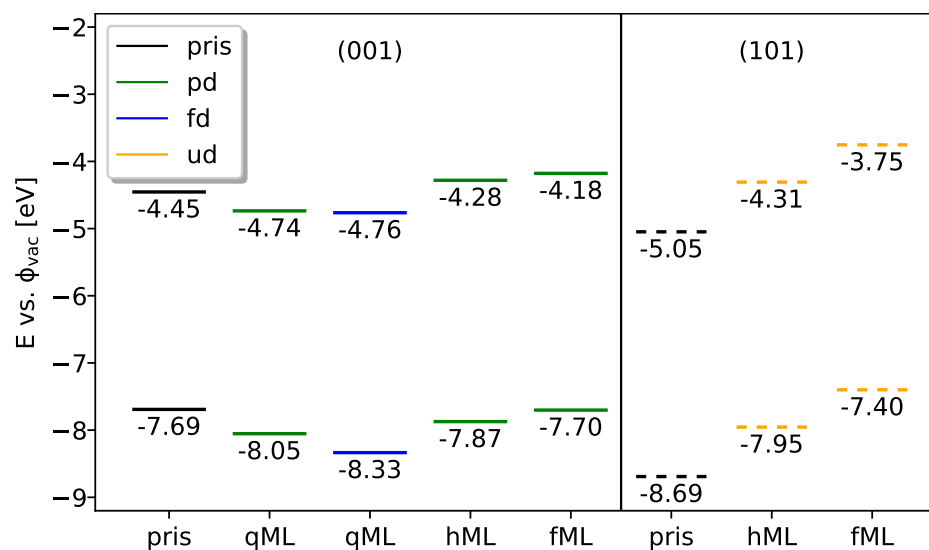211

FIG. 6. Band positions for (001) and (101) surfaces of anatase. VBM and CBM levels are represented as solid and dashed lines, respectively.

212   Our findings are in good agreement with the results of Kashiwaya *et al.* [18], who find a difference

213 in CBM levels of 150 meV to 450 meV. Their values for Fermi level position and VBM are based

214 on photoemission experiments, but as photoemission accesses only occupied states, they had to

215 derive their CBM from an otherwise determined bulk band gap. The Fermi level position in a DFT

216 calculation of a semiconductor is, on the other hand, not very physical and placed on top of the

217 highest occupied state here, so it cannot be compared to the experimental values. This shows that

218 experimental band positions from photoelectron spectroscopy (PES) in vacuum with potentially

219 only partial coverages are expected to deviate significantly from measurements of fully immersed

220 surfaces or from ambient-pressure PES, where thin water layers are conserved. For molecular dy-

221 namics simulations, where timescales are often too short to account for surface chemical reactions,

222 the large band position difference would, in combination with limited slab sizes, lead to large fluc-

223 tuations in the band positions over time. This has indeed been observed by Guo *et al.* [14], where

224 they could not identify a single final model for anatase TiO_2 from the MD simulations alone, albeit

225 already for the (101) surface. Our results suggest that the situation for the (001) surface is even

226 more challenging.

IV. CONCLUSION

228   Our investigations into the (101) and (001) surfaces of anatase in contact with water reveal a

229 rich surface chemistry of anatase, especially in the case of the (001) surface. For both surfaces, we

230 identify considerable variations in the electronic structures and resulting band levels that depend

231 on water coverage and degree of dissociation. These variations can both, improve and diminish

232 the performance of anatase nanocrystals as photocatalysts, by modifying the relative band align-

233 ment as underlying driving force for electron-hole separation. Analysis of the densities of states

234 for the different structures allowed us to identify an occupied, Ti-related surface state for the (001)

235 surface. Its passivation by dissociative adsorption of water plays a crucial role in the observed

236 band level variations. Our results suggest that, especially for the (001) surface, a wide tuning of

237 the band positions and hence charge-transfer properties for both, solid–solid and solid–electrolyte

238 interfaces should be possible by specifically conserving or passivating surface states. Preferen-

239 tial formation of {001} facets can be facilitated in the presence of fluorine ions.[34] The combina-

240 tion with subsequent, selective underpotential deposition[35] of different catalysts or not covalently

241 bonded passivation layers such as graphene (oxide), could then, in principle, allow for the control

of relative band positions. Alternatively, physical methods such as a combination of annealing and oxidation steps can be used to fine-tune the density of surface states[18] and, consequently, also band positions. We expect such modifications to allow for considerable improvements on the performance of anatase-based photocatalysts.

SUPPLEMENTARY MATERIAL

See supplementary material for different views of the relaxed structures as well as local density of states for the topmost layer of the bare (001) surface.

ACKNOWLEDGMENTS

DATA AVAILABILITY STATEMENT

The data that supports the findings of this study are available from the corresponding author upon reasonable request.

REFERENCES

[1] A. Fujishima and K. Honda, Nature **238**, 37 (1972).

[2] B. Neumann, P. Bogdanoff, and H. Tributsch, Journal of Physical Chemistry C **113**, 20980 (2009).

[3] C. N. Sayers and N. R. Armstrong, Surface Science **77**, 301 (1978).

[4] J. P. W. Treacy, H. Hussain, X. Torrelles, D. C. Grinter, G. Cabailh, O. Bikondoa, C. Nicklin, S. Selçuk, A. Selloni, R. Lindsay, and G. Thornton, Physical Review B **95**, 075416 (2017).

267 [5]C. Dette, M. A. Pérez-Osorio, S. Mangel, F. Giustino, S. J. Jung, and K. Kern, Journal of
268 Physical Chemistry C **122**, 11954 (2018).

269 [6]P. J. D. Lindan, J. Muscat, S. Bates, N. M. Harrison, and M. Gillan, Faraday Discussions **106**,
270 135 (1997).

271 [7]S. Selçuk and A. Selloni, The Journal of Physical Chemistry C **117**, 6358 (2013).

272 [8]J. Cheng, X. Liu, J. A. Kattirtzi, J. VandeVondele, and M. Sprik, Angewandte Chemie Interna-
273 tional Edition **53**, 12046 (2014).

274 [9]J. Yu, J. Low, W. Xiao, P. Zhou, and M. Jaroniec, Journal of the American Chemical Society
275 **136**, 8839 (2014), https://doi.org/10.1021/ja5044787.

276 [10]Y. Li and Y. Gao, Physical Review Letters **112**, 206101 (2014).

277 [11]C. E. Patrick and F. Giustino, Physical Review Applied **2**, 014001 (2014).

278 [12]S. Selçuk and A. Selloni, Journal of Physics D: Applied Physics **50**, 273002 (2017).

279 [13]S. Selçuk and A. Selloni, Nature Materials **15**, 1107 (2016).

280 [14]Z. Guo, F. Ambrosio, W. Chen, P. Gono, and A. Pasquarello, Chemistry of Materials **30**, 94
281 (2018), https://doi.org/10.1021/acs.chemmater.7b02619.

282 [15]C. Zhang, J. Hutter, and M. Sprik, Journal of Physical Chemistry Letters **10**, 3871 (2019).

283 [16]Y. He, A. Tilocca, O. Dulub, A. Selloni, and U. Diebold, Nature Materials **8**, 585 (2009).

284 [17]M. Xu, Y. Gao, E. M. Moreno, M. Kunst, M. Muhler, Y. Wang, H. Idriss, and C. Wöll, Physical
285 Review Letters **106**, 138302 (2011).

286 [18]S. Kashiwaya, T. Toupance, A. Klein, and W. Jaegermann, Advanced Energy Materials **8**,
287 1802195 (2018), https://onlinelibrary.wiley.com/doi/pdf/10.1002/aenm.201802195.

288 [19]S. Kashiwaya, J. Morasch, V. Streibel, T. Toupance, W. Jaegermann, and A. Klein, Surfaces **1**,
289 73 (2018).

290 [20]I. Beinik, A. Bruix, Z. Li, K. C. Adamsen, S. Koust, B. Hammer, S. Wendt, and J. V. Lauritsen,
291 Physical Review Letters **121**, 206003 (2018).

292 [21]F. De Angelis, C. Di Valentin, S. Fantacci, A. Vittadini, and A. Selloni, Chemical Reviews **114**,
293 9708 (2014).

294 [22]X.-Q. Gong and A. Selloni, Journal of Physical Chemistry B **109**, 19560 (2005).

295 [23]U. Diebold, Surface Science Reports **48**, 53 (2003).

296 [24]J. Hutter, M. Iannuzzi, F. Schiffmann, and J. VandeVondele, Wiley Interdisciplinary Reviews:
297 Computational Molecular Science **4**, 15 (2014).

298 [25]J. VandeVondele and J. Hutter, Journal of Chemical Physics **127**, 114105 (2007).

[299] [26]C. Hartwigsen, S. Goedecker, and J. Hutter, Physical Review B **58**, 3641 (1998).

[300] [27]J. P. Perdew, K. Burke, and M. Ernzerhof, Physical Review Letters **77**, 3865 (1996).

[301] [28]J. Heyd, G. E. Scuseria, and M. Ernzerhof, The Journal of Chemical Physics **118**, 8207 (2003).

[302] [29]M. Guidon, J. Hutter, and J. VandeVondele, Journal of Chemical Theory and Computation **6**,
[303] 2348 (2010).

[304] [30]A. Selloni, Nature Materials **7**, 613 (2008).

[305] [31]A. Vittadini, A. Selloni, F. P. Rotzinger, and M. Grätzel, Physical Review Letters **81**, 2954
[306] (1998).

[307] [32]A. J. Samin and C. D. Taylor, Applied Surface Science **423**, 1035 (2017).

[308] [33]T. Le Bahers, M. Rérat, and P. Sautet, J. Phys. Chem. C **118**, 5997 (2014).

[309] [34]H. G. Yang, C. H. Sun, S. Z. Qiao, J. Zou, G. Liu, S. C. Smith, H. M. Cheng, and G. Q. Lu,
[310] Nature **453**, 638 (2008).

[311] [35]D. Liang and G. Zangari, Langmuir **30**, 2566 (2014).